



## Full Length Article

# A fully automatic procedure for the analytical reduction of chemical kinetics mechanisms for Computational Fluid Dynamics applications



Quentin Cazères <sup>a,\*</sup>, Perrine Pepiot <sup>b</sup>, Eleonore Riber <sup>a</sup>, Bénédicte Cuenot <sup>a</sup>

<sup>a</sup> CERFACS, 42 Avenue Gaspard Coriolis, Toulouse Cedex 01 31057, France

<sup>b</sup> Sibley School of Mechanical and Aerospace Engineering, Cornell University, NY 14853, United States

## ARTICLE INFO

**Keywords:**

Chemical kinetics reduction

ARCANE

Analytically reduced chemistry

## ABSTRACT

A new software called ARCANE has been developed to address the broad need for compact, computationally efficient chemical models for reactive flow simulations. Based on a new, fully automatic and optimised multi-step reduction methodology, ARCANE's purpose is to provide a convenient and more accessible framework for the analysis and reduction of chemical kinetic mechanisms in the general context of combustion chemistry. The capabilities and performance of the methodology are demonstrated through 3 case studies. First, a classical methane/air system with and without nitrogen/oxygen chemistry is studied as a benchmark. The framework is then applied to a kerosene/air mechanism with a multi-component fuel formulation, showing the ability of the fully automatic method to handle complex chemistry. Finally, the generality of the approach is confirmed by developing reduced chemical models for a hydrocarbon steam cracking process.

## 1. Introduction

Prediction and control of combustion processes, be it their efficiency or resulting pollutant emissions, have never been as critical as they are now. Reactive Computational Fluid Dynamics (CFD) has become an essential tool to advance combustion technologies, as numerical approaches allow to investigate broadly customizable configurations unburdened from practical considerations, and may provide better and deeper insight into phenomena that can be difficult to measure and quantify on a test rig. In order to obtain realistic results for complex problems of interest, for example, kerosene spray flames, numerical simulations typically need to combine several physical fields. In the case of turbulent combustion, the two major fields that need to be brought together are fluid dynamics and chemical kinetics of non-homogeneous mixtures. The increasing number of fuels that are considered to either replace fossil fuels (bio-derived fuels) or enhance their performances (hydrogen addition) makes it critical to include accurate chemical kinetics in CFD in order to properly capture fuel effects. The complete description of chemical kinetics for combustion involves a number of molecular species ranging from a few tens (hydrogen combustion) to several thousands (bio-fuels combustion). Three-dimensional simulations with accurate turbulence description and moderately detailed chemical kinetics would require more computing power than is typically

available and accessible today. Fortunately, most flames features and characteristics of interest can be accurately captured with a relatively small number of species and reactions. By carefully selecting the relevant pathways within the detailed kinetics model, a smaller mechanism can be extracted, rendering the CFD simulations feasible both in term of time and computational resources. In order to make reduced chemistry accessible to the broader CFD community, who may lack expertise in chemical kinetic modelling, the reduction methodology must be formulated in a fully automatic fashion, the sole required input being the user's specific needs for their CFD simulations. As this holds true not only for combustion but also for all fields using chemical kinetics in CFD solvers, the automatic procedure should be made as versatile and generic as possible.

In this work, the new numerical tool ARCANE for the automatic, robust, and user-friendly reduction of chemical kinetic schemes is presented, and its performance is assessed. The individual reduction methods used in ARCANE are first briefly summarised, and their efficient implementation and automation described. The code capabilities are then demonstrated through three different applications of increasing complexity. All computations of chemical properties and canonical cases are performed with the chemistry solver Cantera [1].

\* Corresponding author.

E-mail address: [quentin.cazeres@cerfacs.fr](mailto:quentin.cazeres@cerfacs.fr) (Q. Cazères).

## 2. Reduction methods

The reduction strategy used in this work follows the approach described in Lu et al. [2], and is referred here as the Analytically Reduced Chemistry methodology (ARC). In contrast to other, more intrusive methodologies (e.g. [3–5]), ARC's main advantage is to preserve as much as possible the integrity of the detailed chemical kinetic model: all relevant chemical pathways are included, and there is no kinetic parameter optimisation. Those guiding principles allow for potentially greater robustness in complex simulations and facilitate the chemical interpretation of CFD results.

Reference canonical cases are needed and drive the accuracy of the reduced mechanism with error thresholds applied on specific quantities extracted from those cases. The aforementioned preserved chemical pathways allow for the canonical cases matrix to be quite sparse. Typically, when targeting the evolution of a specific quantity, only a few characteristic points can be selected and not necessarily the whole range. For example, if laminar flame speeds are of interest, only 3 laminar premixed unstrained flames are typically needed (for a given initial temperature and initial pressure): the stoichiometric case and the lean and rich flammability limits, as those 3 cases together will capture all relevant chemical pathways activated at intermediate equivalence ratios.

The three methods combined into ARCANE's multi-step strategy are the Direct Relation Graph with Error Propagation [6] (for both species and reaction reduction), chemical lumping [7], and the Quasi Steady State Approximation [8]. The following sub-sections explain the implementation of the aforementioned methods in ARCANE. The underlying theory is detailed only when the original methods are adjusted for efficiency purposes.

### 2.1. DRGEP

The goal of the first step is to identify the species and the reactions that are not relevant for the set of canonical cases chosen as representative of the target configuration, and can therefore be eliminated from the chemical model with limited loss of accuracy. In this work, DRGEP has been chosen for its generic formulation, which can be applied to a wide range of chemical processes, and for its execution speed compared to other methods (Sensitivity Analysis, or SA, for example [9]).

According to the type of DRGEP reduction, each species or reaction is attributed a coefficient quantifying how strongly it is linked to the targeted quantity of interest. For species, the Direct Interaction Coefficient between a species  $B$  and a target  $A$  is computed for every composition encountered in the canonical simulation:

$$r_{AB} \equiv \frac{\left| \sum_{j=1,n_R} \nu_{j,A} \dot{\omega}_j \delta_B^j \right|}{\max(P_A, C_A)} \quad (1)$$

For reactions, the Direct Interaction Coefficient between reaction  $j$  and target  $A$  is expressed as:

$$r_{Aj} \equiv \frac{|\nu_{j,A} \dot{\omega}_j|}{\max(P_A, C_A)}, \quad (2)$$

where  $n_R$  is the number of reactions in the mechanism,  $\nu_{i,A}$  the stoichiometric coefficient of species  $A$  in the reaction  $j$ ,  $\dot{\omega}_j$  the net rate of progress of reaction  $j$ ,  $C_A$  and  $P_A$  the consumption and production rates of species  $A$ , and  $\delta_B^j$  equals 1 if  $B$  is involved in reaction  $j$ , 0 otherwise. This analysis is performed on all canonical cases computed with the detailed kinetic mechanism under consideration. The temporal and spatial grids used for the computations of the canonical cases are constructed by the Cantera solver in order to sufficiently resolve the species gradients and result in non-uniform grid refined around the high gradients zones.

To accelerate the algorithm, it is applied to a user-defined subset of compositions, obtained using box-filtered values of the test case solutions [6]. The final DRGEP coefficient for each species or reaction is the maximum value over all sample points of all test cases and all target quantities:

$$r_i = \max_{\text{samples,cases,targets } j} r_{ij} \quad (3)$$

The species/reactions are sorted by their DRGEP coefficients in ascending order and progressively removed from the kinetic mechanism, until the error on the target quantities of the canonical cases, recomputed each time, reaches a predefined tolerance.

### 2.2. Chemical lumping

In many detailed mechanisms, especially when dealing with chemical kinetics for heavy hydrocarbons, isomers species can coexist, that is, species with the same molecular composition but different structure and thus thermodynamic properties. Chemical lumping aims at representing a group of isomers using a single representative species, thereby decreasing the number of species and reactions without significantly changing the reactions dynamics.

Candidate species for lumping are automatically identified based on their molecular composition, and the thermodynamic data and kinetic parameters of the reactions involving lumped species are adjusted to account for the larger concentration of the lumped representative. To do so, the relative contribution (in moles) of each isomer species  $i$  to the group of isomers  $I$  is first recorded as a function of the temperature, and the resulting dataset is fitted with an Arrhenius law:

$$X_{I,i}(T) = \frac{X_i}{\sum_{i \in I} X_i} = A_i T^{b_i} \exp^{-\frac{E_{a_i}}{RT}}, i = 1, n_I \quad (4)$$

where  $X_{I,i}(T)$  is the relative mole contribution of isomer  $i$  in its isomer group  $I$ , and  $n_I$  is the number of isomers in the group.

Thermodynamic properties of the lumped isomer, including heat capacity, enthalpy and entropy, are obtained as temperature-dependent, isomer weighted average of the NASA polynomials of each individual isomer. Reaction rates of each reaction involving the lumped representative isomer are also modified to account for the larger concentration of the lumped species, by incorporating the relevant relative mole contributions from Eq. 4 directly into the Arrhenius parameters for that reaction. As an example, consider the case of an isomer  $i$  being lumped into a group of isomers  $I$ . The Arrhenius parameters for a reaction  $j$  involving isomer  $i$  as the only reactant will be modified as follows:

$$\dot{\omega}_j = A_j T^{b_j} \exp^{-\frac{E_{a_j}}{RT}} (X_i) = A_j T^{b_j} \exp^{-\frac{E_{a_j}}{RT}} (X_{I,i}) X_I \quad (5)$$

where  $X_I$  is the mole fraction of the group of isomers  $I$ . Using Eq. 4, one gets:

$$\dot{\omega}_j = (A_j A_i) T^{b_j + b_i} e^{-\frac{E_{a_j} + E_{a_i}}{RT}} X_I, \quad (6)$$

yielding the following modified reaction coefficient  $\tilde{k}_j$ :

$$\tilde{k}_j = (A_j A_i) T^{b_j + b_i} e^{-\frac{E_{a_j} + E_{a_i}}{RT}} \quad (7)$$

with  $\tilde{k}_j$  the modified reaction constant of reaction  $j$ .

### 2.3. Quasi-Steady State assumptions

From a CFD perspective, the Quasi-Steady State Assumption (QSSA) has two major benefits: it removes species and thus leads to fewer transport equations, and it removes numerical stiffness as Quasi-Steady State species are, by definition, species with short characteristic time-scales. To identify QSS candidates among species, a modified Level Of

Importance criterion from Løvås et al. [10] is used:

$$LOI_i = S_{Ti}^S c_i \tau_i, \quad (8)$$

with  $LOI_i$  the Level Of Importance of species  $i$ ,  $S_{Ti}^S$  the sensitivity of species  $i$  to the temperature  $T$ ,  $c_i$  its concentration and  $\tau_i$  the timescale of species  $i$ . As mentioned in 2.1, the sensitivity analysis has not been found to be computer effective and thus an alternative formulation is proposed:

$$LOI_i = r_i c_i \tau_i \quad (9)$$

with  $r_i$  the DRGEP coefficient computed with Eq. 3 and  $c_i \tau_i$  computed as follow:

$$c_i \tau_i = \min_{\text{allsamples}} c_{s,i} \frac{\partial c_{s,i}}{\partial c_{s,i}} \quad (10)$$

which introduces the inverse of the  $ii$  component of the Jacobian matrix of the chemical scheme.

### 3. Automatic procedure

The above algorithm can be fully automated to efficiently reduce any detailed chemical mechanism (in standard Arrhenius format) without the need for expert decisions. The procedure is decomposed into four stages: the number of species is reduced first, followed by a reduction of the number of reactions. Isomer species are then lumped, and Quasi-Steady State assumptions are applied. While each step can be performed independently, the novelty of the ARCANE approach resides in its ability to decide automatically which reduction stage to apply and in which order, thereby delivering *a fully reduced mechanism without requiring any intermediate user input*.

#### 3.1. Automation of each step

##### 3.1.1. Species and reactions reduction

The species and reaction reduction steps are quite simple and similar as they both use DRGEP. At each iteration, one species (or reaction) is discarded from the original, or root, mechanism according to the sorting given by Eq. 3, and the target cases are computed with the resulting reduced mechanism. Iterations are repeated as long as the error on all target quantities stays below the specified tolerance. It may happen that the error goes above the tolerance and then goes back below it at the next iteration. In that case, the smallest mechanism with all errors below the tolerance is taken as the valid reduced mechanism, but the algorithm continues until it reaches a user-specified threshold (2 times the error tolerance for example). This allows to go slightly further in the reduction. To go even further, and considering that the DRGEP algorithm may misplace some species or reactions in the sorted list, those inducing errors that are too high are kept and the reduction continues until reaching species or reactions that cannot be removed, for example major combustion products.

##### 3.1.2. Lumping species

The lumping of chemically similar species is a more complex step as a group of isomers may not always be replaced by a single representative species. Thus, this step is split into 3 sub-steps. First, a check is performed to identify potential species that are strictly identical in both composition and thermodynamic properties, but appearing under different names. Those species are lumped first, as they typically lead to smaller errors. Then, an attempt to lump the whole isomer group is done, now accounting for potential differences in thermodynamic properties. If this leads to errors above the tolerance, lumping the isomers in pairs is finally attempted. The pairs are identified by determining thermodynamic properties (heat capacity, enthalpy, and entropy) similarities between isomers. Two species are deemed similar if the relative

difference between each of their properties remains below 50% for all temperatures between 300 K and 5000 K. Note that fuel species are never considered suitable candidates for lumping.

##### 3.1.3. Quasi Steady State assumptions

The final step of the reduction consists in identifying species that can be considered in quasi-steady state (referred as QSS species in the following). This step is similar to the DRGEP species reduction step. According to the modified LOI criterion of Eq. 9, species are sorted in a list of QSS species. As explained in [11], this step requires to analytically solve a  $Ac = b$  linear system with  $A$  being the  $n_{QSS}^2$  matrix of coupling coefficients between the QSS species,  $c$  the vector of concentrations of the QSS species and  $b$  a vector depending only on the transported, non-QSS species concentrations. The matrix  $A$  is defined as:

$$A_{ik} = - \left( \frac{\sum_{j=1,n_R} \nu'_{ij} k_j}{\sum_{j=1,n_R} \nu'_{ij} k_j} \right) \delta_{ik} \quad i, k = 1, n_{QSS} \quad (11)$$

where  $\nu'_{ij}$  and  $\nu'_{ij}$  are respectively the reactants and products stoichiometric coefficients of species  $i$  in reaction  $j$ ,  $k_j$  the rate constant of reaction  $j$  and  $\delta_{ik}$  equals 1 if  $\nu'_{kj}$  and  $\nu'_{ij}$  are non-zero, i.e., if species  $k$  is consumed in reaction  $j$  to produce  $i$ , else 0.

This set of analytical relations allows to evaluate QSS species concentrations from the non-QSS species concentrations only. The current implementation of the QSS assumption in this work is an extension of the original assumption with an *a posteriori* validation. Here, species that do not fit strictly the theoretical concept may be put in quasi-steady state provided that the targeted characteristics are properly predicted. ARCANE generates and compiles the corresponding equations as a dynamic library file, which can be linked to the reactor or flow solver used to integrate the chemistry.

#### 3.2. Overall automation

Experience shows that the level of reduction that can be achieved for a given error threshold can be much improved by optimising the sequence of the reduction steps, including potential repetitions of individual steps. To the knowledge of the authors, the systematic and automatic reduction sequence optimisation has not been proposed or investigated in the literature.

The first sequence in the optimisation procedure concerns the species and reactions DRGEP steps. Indeed, after each iteration removing a species or a reaction, the graph corresponding to the remaining kinetic network is greatly changed, meaning that the DRGEP coefficients become less and less valid. Performing the DRGEP steps several times may become useful, in order to make sure that the final result is based on correct DRGEP coefficients which are re-computed at each step. In ARCANE, species and reaction reduction is done as part of an iterative loop, and repeated alternatively until no further change is observed. The DRGEP loop is illustrated in Fig. 3.1.

The initial DRGEP loop is followed by a lumping step. Since the lumping does reorganise the kinetic network significantly, the DRGEP loop of Fig. 3.1 is repeated a second time. Once this second loop is done, the QSS reduction step is finally performed. The reduced mechanism returned by this last step is the final result of the whole reduction process.

#### 4. Encapsulating code structure

The automatic reduction algorithm has been implemented in ARCANE (for Analytically Reduced Chemistry: Automatic, Nice and Efficient) which fully exploits the object-oriented nature of Python by revolving around two major objects that contain all the necessary information. The first object, referred as the Case object, is carrying all the

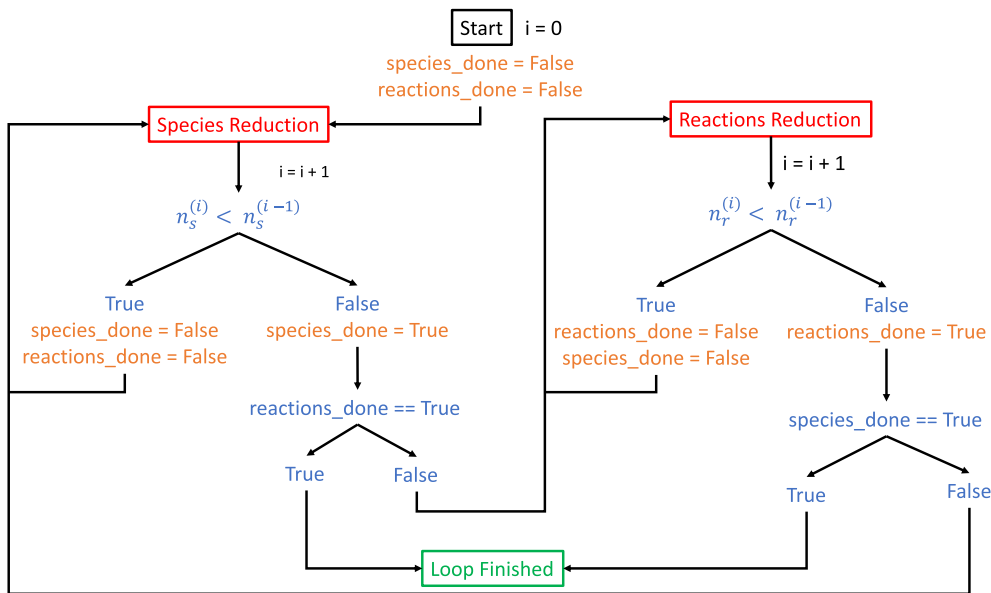


**Fig. 3.1.** Schematic of the loop between species reduction and reactions reduction steps with  $n_s^{(i)}$  and  $n_r^{(i)}$  respectively, the number of species and the number of reactions in the mechanism generated at the  $i$ -th reduction iteration.

operating conditions such as the type of canonical reactor to simulate, the composition of the mixture, and all other parameters necessary for the computation, independently of the mechanism to use. The second object, referred as the Mechanism object, is carrying the information about the mechanism. For each step of the reduction, the reduced Mechanism object is passed to the Case objects to be recomputed and compared to the results with the detailed mechanism. This structure with uncoupled objects allows a great flexibility in the cases that can be computed and the number of mechanisms that can be used. The data resulting from the computation of a case with a given mechanism is stored in a database structured as shown in Fig. 4.1. The systematic storage of the generated data in a formatted shape allows to re-use already existing data, thereby saving time if restarting a reduction or analysing results. The compositions sampled from the canonical simulation, mentioned in Section 2.1, are then used in the reduction steps with each case treated independently with its specific targets, before concatenating the results to obtain the final reduction result.

In principle, ARCANE may use any 0D/1D combustion solver. In its current version, ARCANE is coupled with the open-source software Cantera [1]. Cantera offers a wide range of options when dealing with chemical kinetics computations, from reactor networks to various one-dimensional flames going from the simplest configurations (freely propagating premixed flames, counter-flow diffusion flames) to more complex ones (ionic premixed burners, or impinging jets).

## 5. Capabilities

Besides complete automation, the other innovation of the method is its versatility resulting from the large variety of canonical computations that may be used to represent real-life processes. The present method has been designed to be able to work with any kind of dataset provided that temperature, pressure, and species concentrations are available. Another flexibility that proved to be useful is the possibility to assign different tolerances for the various quantities targeted in a single case (for example, a 5% error threshold on laminar flame speed and 1% error on maximum temperature can be applied in the same case).

To demonstrate the capabilities of ARCANE, three different case studies are presented in the remainder of this paper. The first one is an ubiquitous configuration in the combustion community: the reduction of a methane/air mechanism with and without NO<sub>x</sub> predictions. The purpose of this test case is to serve as a benchmark and demonstrate the

performance of the proposed automatic procedure through comparison with literature results. The second case study is the reduction of a three-components surrogate of kerosene, aiming to show the code performance on a complex mechanism with a high number of species and reactions. Finally, the third case study explores a non-combustion configuration, and considers butane steam-cracking. This last case demonstrates the validity and adequacy of the method for any kind of chemical process.

### 5.1. Reduction of Methane/air combustion chemistry

Methane being the simplest hydrocarbon and the major component of natural gas, used in ground-based gas turbines and furnaces, it has been widely studied in the literature. Mainly using GRI-Mech [12] as the detailed reference mechanism, numerous chemistry reductions have been proposed (e.g. [13–15]). Among them, the two reduced mechanisms developed by Lu et al. [16] with and without NO<sub>x</sub> predictions are quite popular and as such, were used in [17] as references to assess the validity of reduced mechanisms obtained with the same techniques as those implemented in ARCANE [11]. They are therefore also used here to benchmark the present algorithm.

#### 5.1.1. Methane/air chemistry reduction without NO<sub>x</sub> chemistry

The 19 species, 11 QSS species and 184 reactions <sup>1</sup> mechanism of [16] is used here as the reference and referred in the following as Lu19. This mechanism was obtained with an error threshold of 10% in auto-ignition cases and Perfectly Stirred Reactors (PSR). In the present study, different error thresholds are applied depending on the case, as summarised in Table 5.1. On every case, the target was chosen to be only the heat release rate.

ARCANE produced a 16 species, 129 reactions and 10 QSS species mechanism. The complete reduction took around 30 min on a PC, from which 67% was spent on the computation of the cases by Cantera. Fig. 5.1 represents the series of reduction steps followed from the detailed mechanism to the final ARC scheme. For this relatively simple

<sup>1</sup> not to be confused with the 15 steps presented by the authors [18], and representing the number of elemental reactions that do not involve QSS species. Using the same numbering of reactions as in the present work, the mechanism counts 368 irreversible reactions.

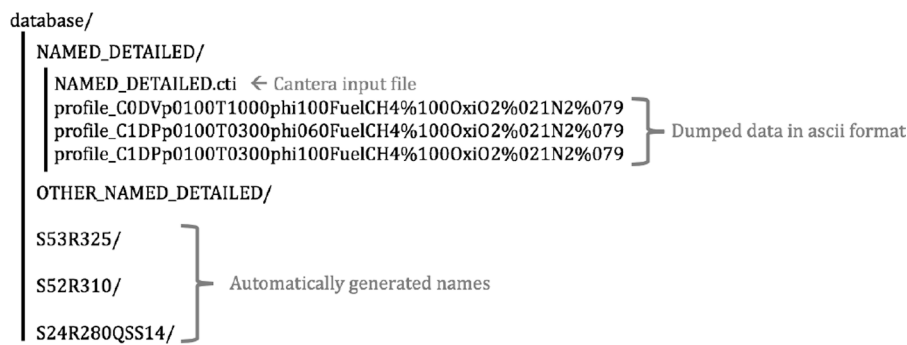


Fig. 4.1. Structure of the database directory.

Table 5.1

Definition of the two considered canonical cases and associated error thresholds applied to various quantities for the methane-air chemistry reduction without  $\text{NO}_x$  chemistry.

Reactor type	0D Isochoric reactor	1D premixed flame
Temperature [K]	1000, 2000	300
Pressure [bar]	1	1
Equivalence ratio	1	0.5, 1, 1.5
Error threshold on Auto-ignition delay time	5%	/
Error threshold on Laminar flame speed	/	2%
Error threshold on Maximum temperature	1%	1%

chemistry, the reduction process is straightforward with only one repetition of the species reduction step. The obtained mechanism (referred in the following as Cazeres16) is compared to the detailed mechanism (GRI-Mech 3.0) and Lu19 for laminar flame speeds and ignition delay times over a wide range of conditions. No significant differences can be seen between the three mechanisms, even though the present mechanism Cazeres16 is more reduced than the Lu19.

The difference between Lu19 and Cazeres16 in terms of species is summarised in Table 5.2. Interestingly, the present reduction seems less

strict for the fastest species, removing some QSS species that are kept in Lu19, and treating as QSS some species that are still transported in Lu19. Note the particular case of  $\text{CH}_2\text{CO}$ , which is transported in Lu19 but removed in Cazeres16, without any degradation of the results.

### 5.1.2. Reduction with $\text{NO}_x$

Adding the prediction of  $\text{NO}_x$  through the addition of the  $\text{NO}$  and  $\text{NO}_2$  species as targets, and using the test cases and thresholds of Table 5.3 on the GRI-Mech 2.11 detailed mechanism, ARCANE led to a mechanism consisting of 22 transported species, 140 reactions, and 14 QSS species, that is, 6 additional transported species and 4 additional QSS species compared to Cazeres16. This reduction was slightly longer and took 45 min on a PC, from which 87% was devoted to the computation of the

Table 5.2  
Species differences between Lu19 and Cazeres16.

Species	Status in Lu19	Status in Cazeres16
$\text{C}_2\text{H}_2$	transported	QSS
$\text{CH}_3\text{OH}$	transported	QSS
$\text{CH}_2\text{CO}$	transported	removed
C	QSS	removed
$\text{C}_2\text{H}_3$	QSS	removed
HCCO	QSS	removed

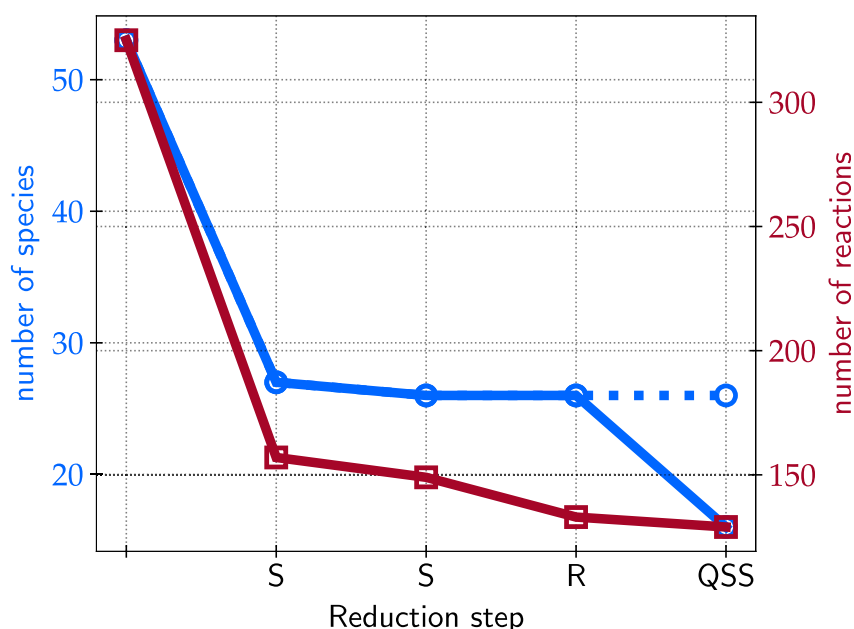


Fig. 5.1. Graphical representation of the methane/air chemistry without  $\text{NO}_x$  reduction process: number of species (solid blue line with circles: transported species, dashed blue line with circles: all species) and number of reactions (red line with squares). On the abscissa axis, 'S' stands for species reduction step, 'R' for reactions reduction step and 'QSS' for Quasi-Steady State approximation step.

**Table 5.3**

Definition of the two canonical cases considered in the study and associated error thresholds applied to various quantities for the methane-air reduction with  $\text{NO}_x$  chemistry.

Reactor type	0D Isochoric reactor	1D premixed flame
Temperature [K]	1000, 2000	300
Pressure [bar]	1	1
Equivalence ratio	1	0.6, 1, 1.4
Error threshold on Auto-ignition delay time	5%	/
Error threshold on Laminar flame speed	/	2%
Error threshold on Maximum temperature	1%	1%
Error threshold on NO mass fraction integral	5%	5%

flame cases (see Fig. 5.2). As shown in Fig. 5.3, for this case, several successive repetitions of the same reduction step were necessary, especially for the reduction of reactions which ended in an important number of discarded reactions. Note also the additional species reduction step after the reactions reduction, which allowed a significant further decrease of the species number because of significant changes in the reaction paths graph. This mechanism (referred in the following as Cazeres22) is compared to the detailed mechanism GRI-Mech 2.11. The reason why this mechanism was used instead of the GRI-Mech 3.0 is because it was found to have a better prediction of  $\text{NO}_x$  emissions in previous studies [17]. The present mechanism was found to be very similar to the latter study, having 4 additional QSS species (C, HCCO, HCNO, NCO) and the same 22 transported species as Cazeres22.

Fig. 5.5 shows that Cazeres22 recovers all the target quantities across the range of equivalence ratios, as well as the  $\text{NO}_2$  mass fraction integral except for the very rich part of the curve. Note that the slight increase in the NO mass fraction integral error occurs in a region where the absolute value of NO is low, and is therefore not overly concerning.

Compared to Cazeres16, there are 6 additional transported species namely NO,  $\text{NO}_2$ ,  $\text{N}_2\text{O}$ , HCN,  $\text{C}_2\text{H}_2$ ,  $\text{CH}_3\text{OH}$ . Naturally, NO and  $\text{NO}_2$  are kept because they are the species of interest in this case.  $\text{N}_2\text{O}$  and HCN are transported as important species in the  $\text{NO}_x$  emission process, with an influence on the chemical dynamics too important to be put in quasi-steady state.  $\text{C}_2\text{H}_2$  and  $\text{CH}_3\text{OH}$  were set in quasi-steady state in Cazeres16 but are now being transported. This indicates that they need to be included to reproduce the correct combustion behaviour, but their correct prediction becomes critical when  $\text{NO}_x$  are involved. There are 4 more QSS species in Cazeres22 compared to Cazeres16, but this difference is actually an addition of 8 new QSS species with a discarding of 4 former QSS species. The species added are all species with nitrogen atoms directly linked to the  $\text{NO}_x$  emissions (N, NH,  $\text{NH}_2$ ,  $\text{NNH}$ , HNO, HOCH, HNCO) except for  $\text{C}_2\text{H}_3$ . From the 4 discarded species,  $\text{C}_2\text{H}_2$  and  $\text{CH}_3\text{OH}$  were moved to the transported species list and  $\text{CH}_2\text{OH}$  and  $\text{CH}_2\text{CHO}$  were completely discarded from the mechanism. The addition of  $\text{C}_2\text{H}_3$  can be explained by the need for this species to be present to predict  $\text{C}_2\text{H}_2$  more accurately. The reactions involving  $\text{CH}_2\text{OH}$  and  $\text{CH}_2\text{CHO}$  included in Cazeres16 are reactions consuming O, H, and  $\text{O}_2$ . When  $\text{NO}_x$  are involved, those species are predominantly used in  $\text{NO}_x$ -related pathways, rendering those previous consumption routes negligible and leading to  $\text{CH}_2\text{OH}$  and  $\text{CH}_2\text{CHO}$  being discarded from the mechanism. (see Fig. 5.4).

## 5.2. Reduction of kerosene combustion using a three-component surrogate

For industrial applications in the domain of aeronautics, accurate prediction of the combustion of kerosene (Jet-A1 more particularly in that case) is required. Kerosene consists in hundreds of hydrocarbons molecules with an exact composition varying from batch to batch. In the literature, surrogates have been formulated in order to represent the composition of such complex fuels. The one used in this study, taken

from Humer et al. [19], is composed (in volume) of 60% of n-dodecane ( $n\text{-C}_{12}\text{H}_{26}$ ), 20% of methyl-cyclohexane ( $\text{CH}_3\text{C}_6\text{H}_{11}$ ), and 20% of xylene<sup>2</sup> ( $((\text{CH}_3)_2\text{C}_6\text{H}_4$ ). The detailed mechanism employed in this work is taken from Ranzi et al. [20] and is available from their website [21]. This mechanism is labelled CRECK\_2003\_TOT\_HT in the following<sup>3</sup>.

The CRECK\_2003\_TOT\_HT mechanism has been designed to incorporate most species involved in jet fuel combustion and is ideally suited to explore kerosene multi-component surrogates, including the 3-component Jet A1 surrogate of interest in this study. It is based on the concept of a palette of fuel components, individually validated, allowing a variety of surrogates to be simulated. It consists of 368 species among 14,462 reactions. This mechanism does not include low temperature chemistry and is therefore not able to capture the Negative Temperature Coefficient ignition behaviour found at low temperatures. For that reason, only 0D reactors with an initial temperature above 900 K will be computed. For the reduction, heat release rate is targeted along with each individual fuel components. The reduction cases and their relative thresholds are summarised in Table 5.4.

The reduced mechanism obtained with ARCANE consists in 39 species, 276 reactions, and 15 QSS species (referred in the following as Cazeres39).

The reduction process is illustrated in Fig. 5.6. After the first step, which drastically reduces the number of species and reactions, the reduction continues to progressively decrease the number of reactions, until the reaction graph has sufficiently changed to trigger another decrease of species. This process is similar to the methane-air with  $\text{NO}_x$  reduction, only more complex. Compared to methane reduction, a lumping step is now present. Because of the higher number of carbon atoms in the fuel, many isomer species can now be found in the chemical pathways. Not all isomer species are lumped together as isomers can have a very different chemical path and cannot be lumped together. In that case, 3 groups of isomers were identified and successfully lumped together, decreasing the number of transported species by 3.

Although it has not been derived based on individual fuel component combustion, results for flame speeds (Fig. 5.7) and ignition delay time (Fig. 5.8) are shown for the 3-component fuel as well as for the single component fuels.

Results for the 3-component surrogate are in very good agreement with the detailed mechanism, both for laminar flame speed and ignition delay time. For single component fuels, the agreement between detailed and reduced mechanisms is logically related to its proportion in the surrogate blend that was used for reduction. With a mean error of 115% (maximum of 195%) on ignition delay time, and 27% (maximum of 42%) on laminar flame speed, xylene shows the largest error as it is the least present species in mass in the surrogate (13.7% in mass). Indeed, its contribution to the overall heat release rate of the surrogate combustion is low and its specific chemical pathways are marginalised during the reduction process, possibly removed ultimately. Because the reduction is only constrained by the surrogate characteristics, the overall importance of each of its components will be weighted by their relative mass in the fuel mixture. However minor components may be important, for example in two-phase combustion where preferential evaporation may segregate the vapour components. In such case, single component fuel burning should be added to the target cases for the reduction.

It is here important to highlight the significant gain in computational time brought by reduced chemistry: compared to the detailed mechanism, the Cazeres39 scheme allows to reach a speed-up factor of 363 for the computation of the 3-component stoichiometric freely propagating flame.

<sup>2</sup> There is no distinction between xylene isomers (meta-, para-, ortho-xylene) as there is none in the detailed mechanisms

<sup>3</sup> From the detailed mechanisms' authors naming convention, "2003", the mechanism's version, corresponds to March 2020, the latest available update at the time of this study.

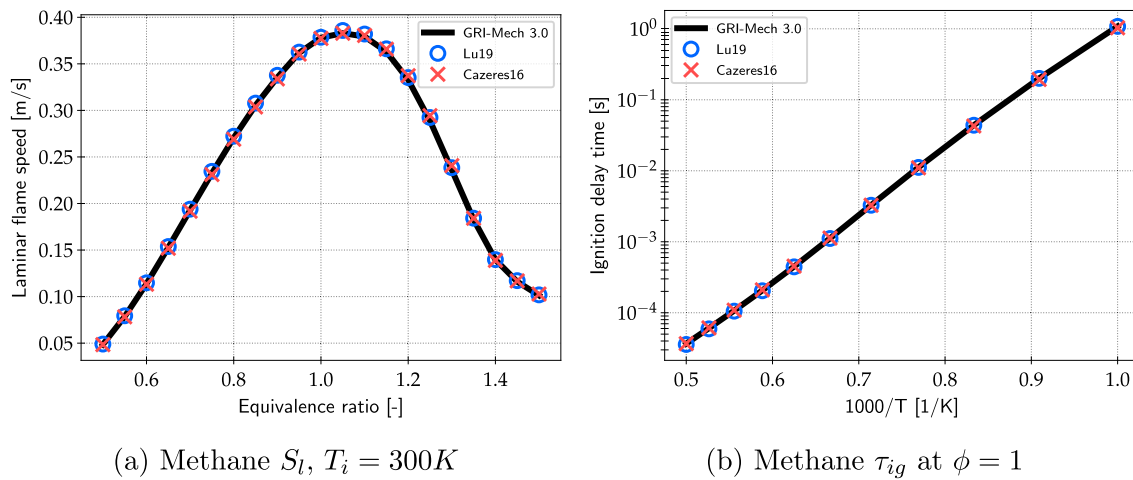


**Fig. 5.2.** Laminar flame speed as a function of the equivalence ratio at 1 bar for (a) methane/air without  $\text{NO}_x$  flames, and (b) methane/air ignition delay time as a function of  $1000/T$  at stoichiometry and 1 bar. Comparison between GRI-Mech 3.0 (black line), Lu19 (blue circles) and Cazeres16 (red crosses).

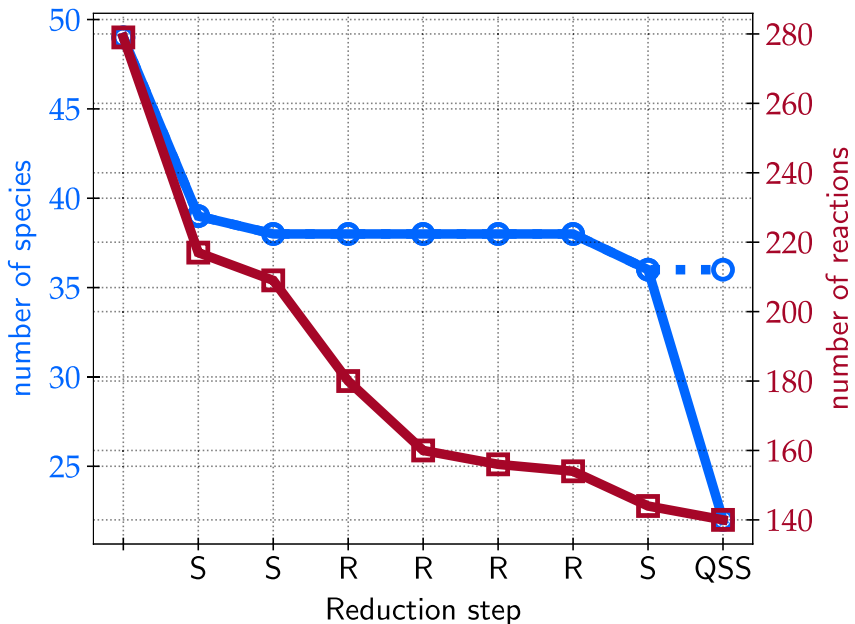


**Fig. 5.3.** Graphical representation of the methane/air chemistry with  $\text{NO}_x$  reduction process: number of species (solid blue line with circles: transported species, dashed blue line with circles: all species) and number of reactions (red line with squares). On the abscissa axis, 'S' stands for species reduction step, 'R' for reactions reduction step and 'QSS' for Quasi-Steady State approximation step.

### 5.3. Reduction of butane steam cracking

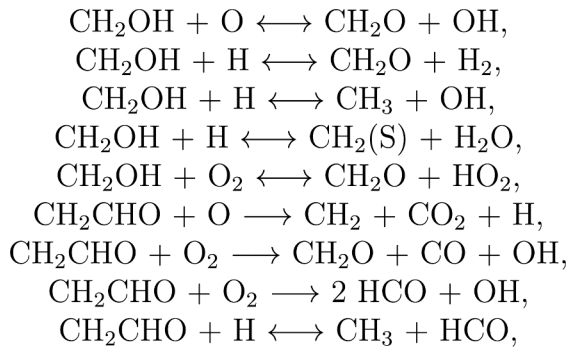
Aside from combustion, the present methodology is suitable for the reduction of kinetic mechanisms applied to any kind of reacting flow process. The simulation of butane steam-cracking, which occurs in high-Reynolds heated pipe flows [22], is one example of application where the use of reduced chemistry is of high interest. First reduction attempts were presented in [23]. Improved results obtained with ARCANE are presented here.

The detailed mechanism is the same as the one used for kerosene combustion and presented in the previous section, without molecules containing more than 4 carbon atoms, leading to a reference detailed mechanism of 181 species and 5554 reactions. The same steam cracking process studied in [23] is chosen for the present study. It is represented by a zero-dimensional constant pressure reactor, heated via a constant heat flux of  $19.38 \text{ MW/m}^3$ . The mixture of 69% of butane and 31% of water vapour (in mass fraction) is initially at 909 K and 2.3 bar. The

simulation is stopped after 0.14s, which is representative of the residence time in butane cracking applications. The main olefins produced by this process are  $\text{C}_2\text{H}_4$ ,  $\text{C}_3\text{H}_6$ , and  $\text{C}_4\text{H}_6$ , and are therefore the quantities on which the controlling error is imposed, with a 1% error threshold applied on the value reached at the end of the simulation.

Based on this test case and tolerances, ARCANE allowed to reduce the mechanism down to 24 transported species, 413 reactions, and 12 QSS species (referenced in the following as Cazeres24).

The reduction process illustrated in Fig. 5.9 shows a relatively simple procedure, with only one repetition of the species reduction and a lumping step. No reaction reduction was necessary in this case meaning that all the reductions not discarded along species are relevant for this application. Main species profiles shown in Fig. 5.10 show a very good agreement between Cazeres24 and the detailed mechanism over the whole simulation, with a maximum deviation of 0.83% on the peak value of butadiene.

Fig. 5.4. Reactions involving  $\text{CH}_2\text{OH}$  and  $\text{CH}_2\text{CHO}$ .

## 6. Conclusions

The proposed methodology for the automated reduction of chemical kinetic mechanisms has been shown to be effective on 3 different mechanisms. First, on the GRI-Mech (3.0 and 2.11) with slightly better results than in the literature, both with and without  $\text{NO}_x$  predictions. It has then shown good performances on the reduction of a Jet A1 3-component surrogate, generating a computationally efficient and affordable 39 species reduced mechanism, despite originating from a 368 species detailed mechanism. Finally, the versatility of the method has been demonstrated on a butane steam-cracking case with perfect

Table 5.4

Definition of the two canonical cases considered in the study, and associated error thresholds applied to various quantities for the three-component kerosene-air reduction.

Reactor type	0D Isochoric reactor	1D premixed flame
Temperature [K]	1000, 2000	400
Pressure [bar]	1	1
Equivalence ratio	1	0.6, 1, 1.4
Error threshold on Auto-ignition delay time	5%	/
Error threshold on Laminar flame speed	/	5%
Error threshold on Maximum temperature	1%	1%

agreement between the 24 species reduced mechanism and its 181 species parent mechanism. The implemented algorithm allows to reduce any given chemical mechanism that can be written in elementary reactions following Arrhenius laws, while controlling the error on any user-defined quantity, either directly available in the computation (concentrations, temperature, pressure etc.) or computed with a user-defined function prescribed as an input to the case object. The current implementation also allows for the addition of other reduction and analysis methodologies, for example based on sensitivity coefficients. The reduced mechanisms derived in this work are freely available in Cantera format in the mechanisms database on the CERFACS website (<https://chemistry.cerfacs.fr/en/home/>) with their associated fortran

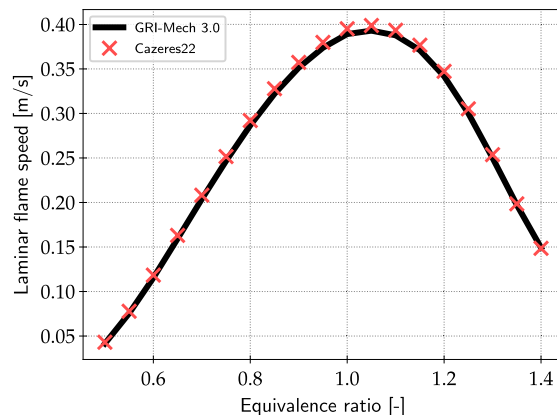
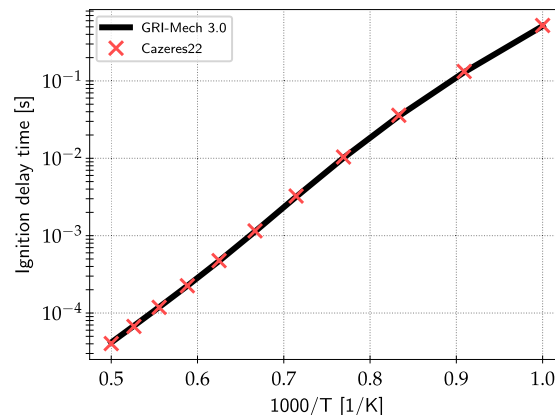
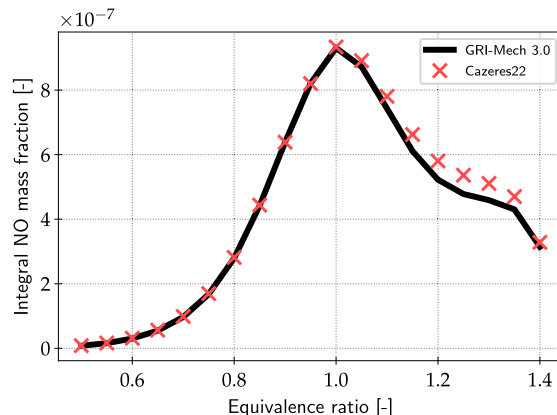
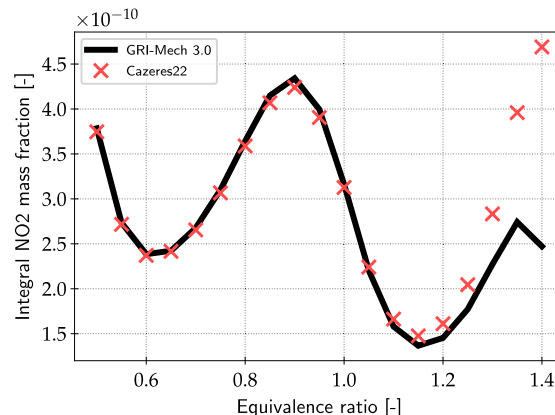
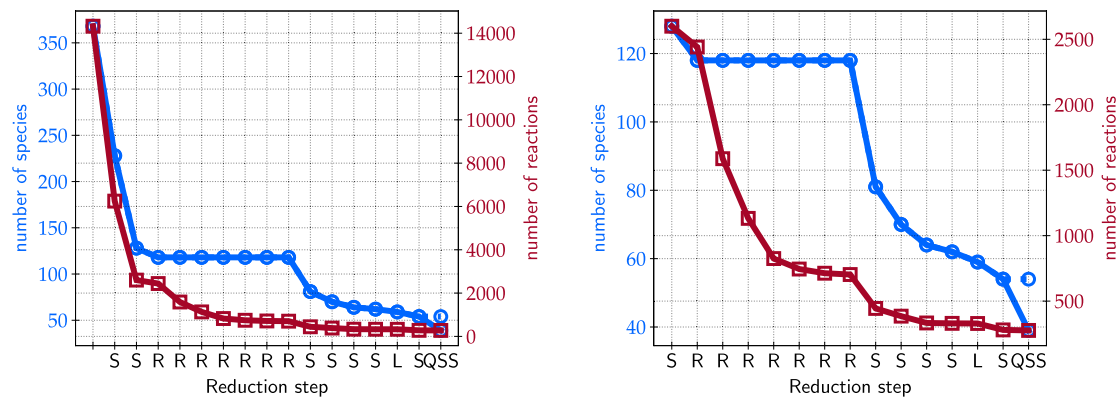
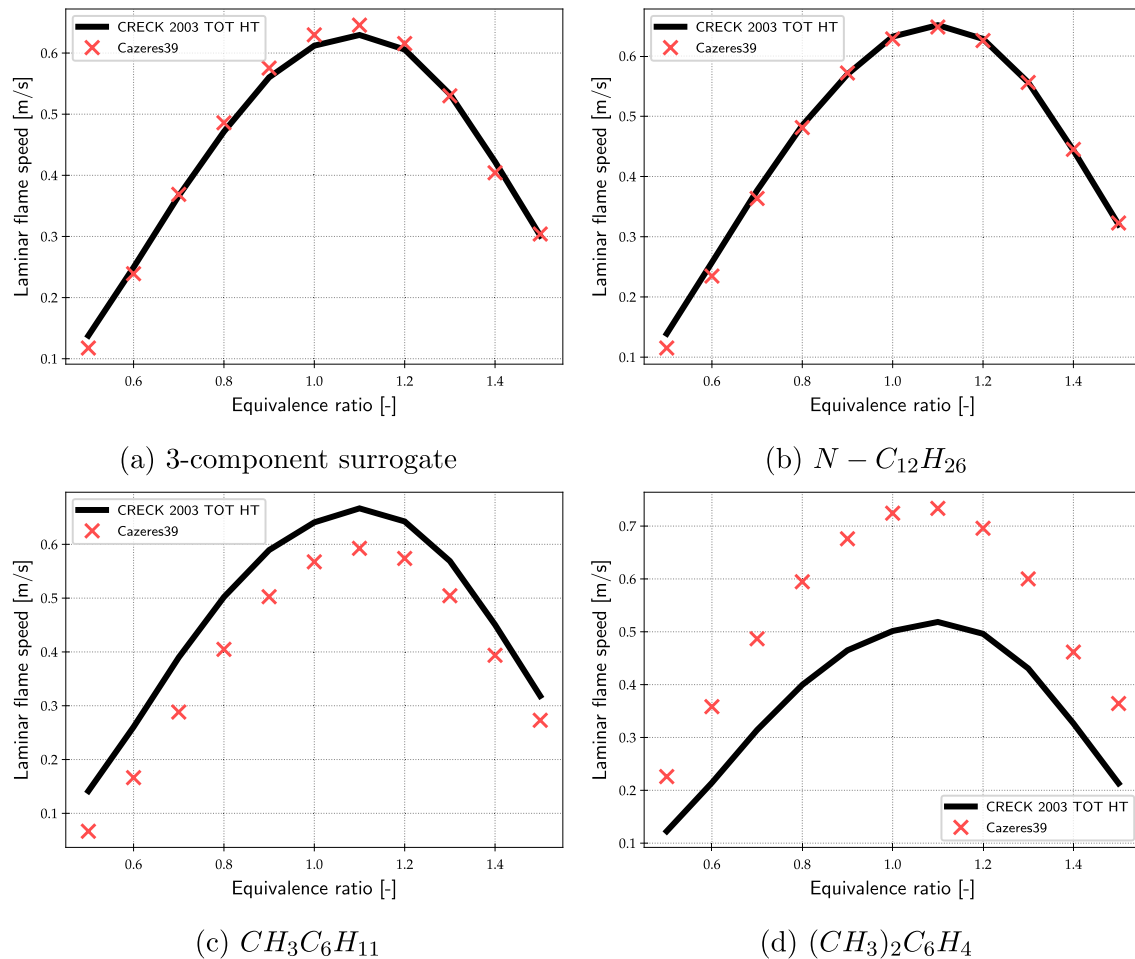
(a)  $S_l$ ,  $T_i = 300\text{K}$ (b)  $\tau_{ig}$  at  $\phi = 1$ (c) NO mass fraction integral,  $T_i = 300\text{K}$ (d)  $\text{NO}_2$  mass fraction integral,  $T_i = 300\text{K}$ 

Fig. 5.5. Methane/air combustion at 1 bar: (a) laminar flame speed as function of the equivalence ratio; (b) ignition delay time as a function of  $1000/T$  at stoichiometry; (c) total NO, and (d) total  $\text{NO}_2$  mass fractions as functions of the equivalence ratio. Comparison between GRI-Mech 2.11 (black line), Cazères22 (red crosses).



**Fig. 5.6.** Graphical representation of the three-component kerosene-air chemistry reduction process: number of species (solid blue line with circles: transported species, dashed blue line with circles: all species) and number of reactions (red line with squares). On the abscissa axis, 'S' stands for species reduction step, 'R' for reactions reduction step, 'L' for lumping step and 'QSS' for Quasi-Steady State approximation step. Left: overall procedure. Right: zoom on the reduction after the first step.



**Fig. 5.7.** Kerosene combustion at 1 bar and 400 K: (a) laminar flame speed as function of the equivalence ratio for the 3-component surrogate, (b) dodecane only, (c) methyl-cyclohexane only, and (d) xylene only. Comparison between CRECK\_2003\_TOT\_HT (black line) and Cazeres39 (red crosses).

mechanisms for computation with QSS species. The CHEMKIN files of the skeletal mechanisms (the QSS implementation being code specific) are available as Supplementary Material. The ARCANE code is available

upon request and the procedure for accessing it is detailed on its specific section of the website.

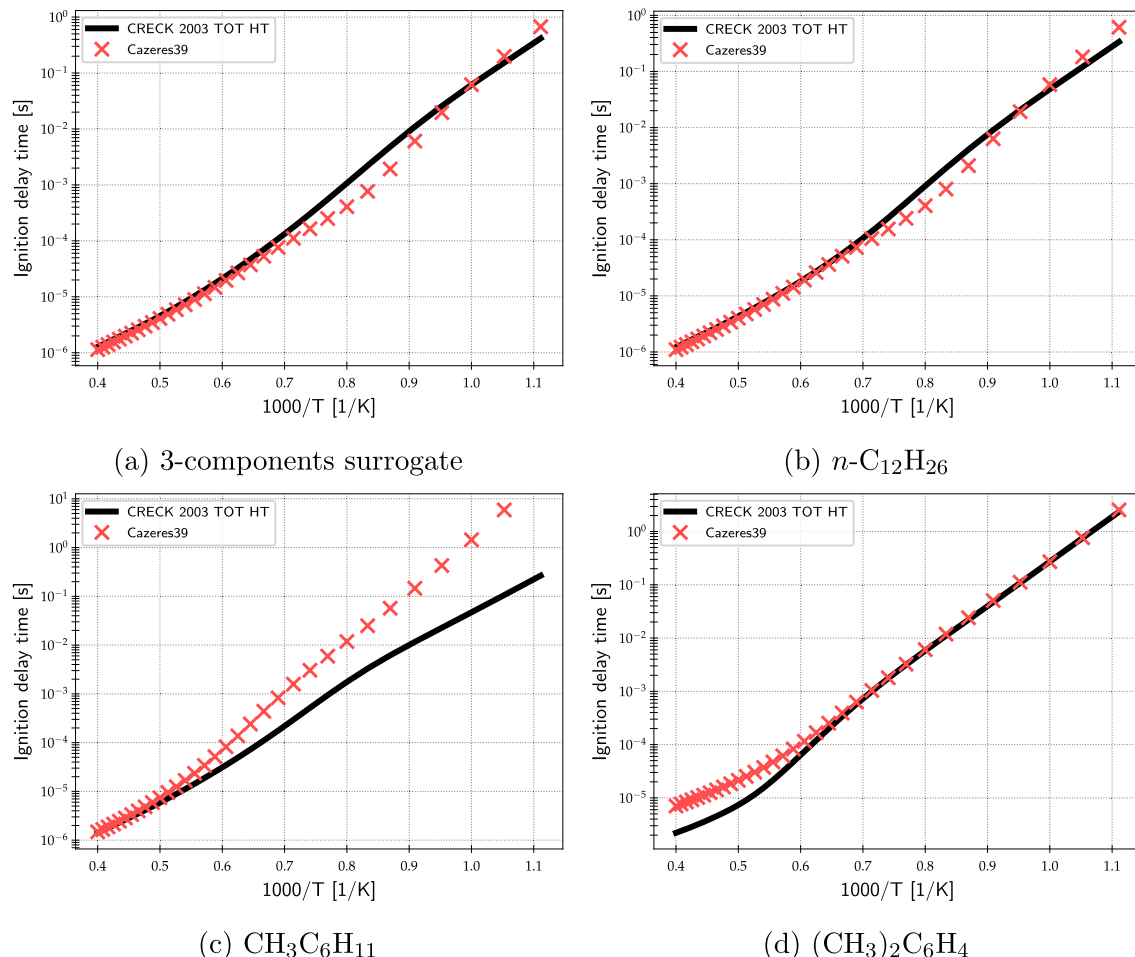


**Fig. 5.8.** Kerosene combustion at 1 bar and 400 K: (a) ignition delay time as a function of  $1000/T$  at stoichiometry for the 3-components surrogate, (b) dodecane only, (c) methyl-cyclohexane only, and (d) xylene only. Comparison between CRECK\_2003\_TOT\_HT (black line) and Cazères39 (red crosses).

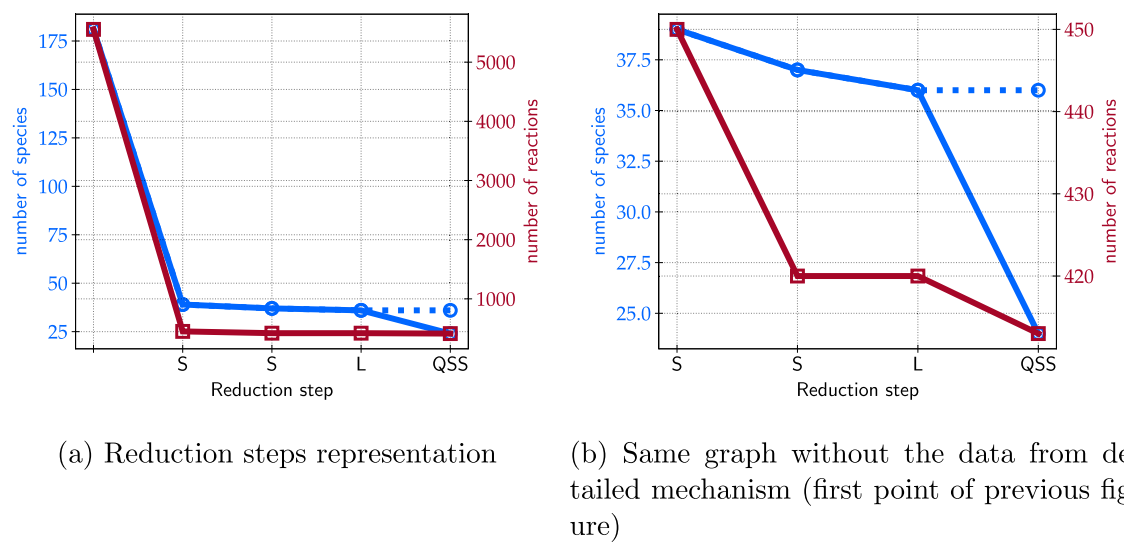


**Fig. 5.9.** Graphical representation of the butane steam-cracking reduction process: number of species (solid blue line with circles: transported species, dashed blue line with circles: all species) and number of reactions (red line with squares). On the abscissa axis, 'S' stands for species reduction step, 'L' for lumping step and 'QSS' for Quasi-Steady State approximation step. Left: overall procedure. Right: zoom on the reduction without the initial.

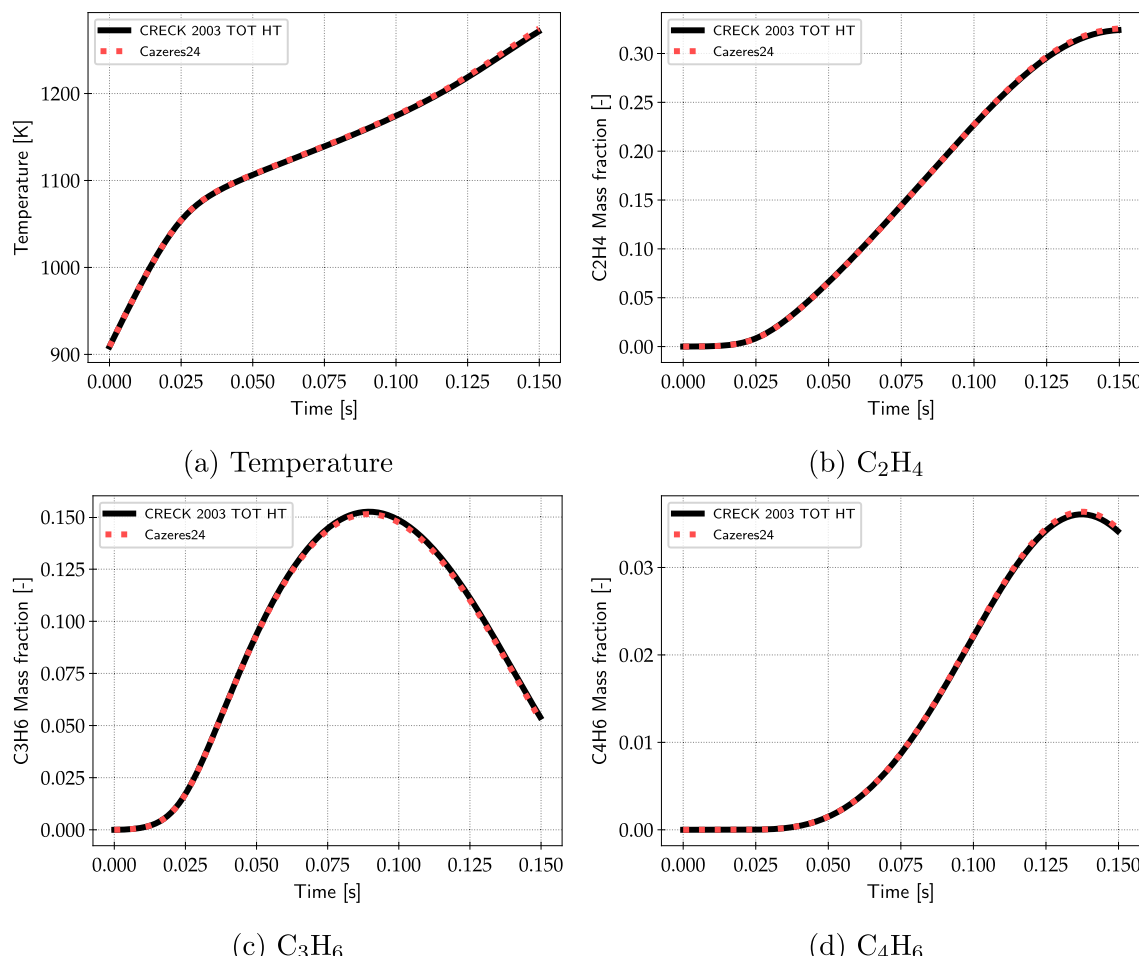


**Fig. 5.10.** Butane steam-cracking: (a) temperature, (b) ethene, (c) propene, and (d) butadiene mass fractions as functions of time. Comparison between CRECK\_2003\_TOT\_HT (black line) and Cazères24 (red dots).

#### CRediT authorship contribution statement

**Quentin Cazères:** Software, Methodology, Validation, Writing - original draft. **Perrine Pepiot:** Software, Methodology, Conceptualization, Writing - review & editing. **Eleonore Riber:** Methodology, Supervision, Writing - review & editing. **Bénédicte Cuenot:** Methodology, Supervision, Writing - review & editing.

#### Declaration of Competing Interest

The authors declare that they have no known competing financial interests or personal relationships that could have appeared to influence the work reported in this paper.

#### Acknowledgement

The authors want to thank Jonathan Wirtz<sup>a</sup>, Theo Ogier<sup>a</sup>, Antoine Pestre<sup>a</sup> and Manqi Zhu<sup>a</sup> for their help. This project has received funding from the European Union's Horizon 2020 research and innovation programme under Agreement 723525 (JETSCREEN).

#### References

- [1] Goodwin DG, Moffat HK, Speth RL, Cantera: An object-oriented software toolkit for chemical kinetics, thermodynamics, and transport processes, <http://www.cantera.org>, version 2.3.0 (2017). doi:10.5281/zenodo.170284.
- [2] Lu T, Law CK. Toward accommodating realistic fuel chemistry in large-scale computations. *Prog Energy Combust Sci* 2009;35(2):192–215. <https://doi.org/10.1016/j.pecs.2008.10.002>. URL: <https://linkinghub.elsevier.com/retrieve/pii/S036012850800066X>.
- [3] Abou-Taouk A, Farcy B, Domingo P, Vervisch L, Sadasivuni S, Eriksson L-E. Optimized reduced chemistry and molecular transport for large eddy simulation of partially premixed combustion in a gas turbine. *Combust Sci Technol* 2016;188(1): 21–39. <https://doi.org/10.1080/00102202.2015.1074574>. <http://www.tandfonline.com/doi/full/10.1080/00102202.2015.1074574>.
- [4] Fiorina B, Viequelin R, Auzillon P, Darabiha N, Gicquel O, Veynante D. A filtered tabulated chemistry model for LES of premixed combustion. *Combust Flame* 2010; 157(3):465–75. <https://doi.org/10.1016/j.combustflame.2009.09.015>. URL: <https://linkinghub.elsevier.com/retrieve/pii/S0010218009002739>.
- [5] Cailler M, Darabiha N, Veynante D, Fiorina B. Building-up virtual optimized mechanism for flame modeling. *Proc Combust Inst* 2017;36(1):1251–8. <https://doi.org/10.1016/j.proci.2016.05.028>. URL: <https://linkinghub.elsevier.com/retrieve/pii/S1540748916300281>.
- [6] Pepiot-Desjardins P, Pitsch H. An efficient error-propagation-based reduction method for large chemical kinetic mechanisms. *Combust Flame* 2008;154(1–2): 67–81. <https://doi.org/10.1016/j.combustflame.2007.10.020>. URL: <https://linkinghub.elsevier.com/retrieve/pii/S0010218007003264>.
- [7] Pepiot-Desjardins P, Pitsch H. An automatic chemical lumping method for the reduction of large chemical kinetic mechanisms. *Combust Theor Model* 2008;12(6):1089–108. <https://doi.org/10.1080/13647830802245177>. URL: <http://www.tandfonline.com/doi/abs/10.1080/13647830802245177>.
- [8] Lu T, Law CK. Systematic approach to obtain analytic solutions of quasi steady state species in reduced mechanisms. *J Phys Chem A* 2006;110(49):13202–8. <https://doi.org/10.1021/jp064482y>. URL: <https://pubs.acs.org/doi/10.1021/jp064482y>.
- [9] Stagni A, Frassoldati A, Cuoci A, Faravelli T, Ranzi E. Skeletal mechanism reduction through species-targeted sensitivity analysis. *Combust Flame* 2016;163: 382–93. <https://doi.org/10.1016/j.combustflame.2015.10.013>. URL: <https://linkinghub.elsevier.com/retrieve/pii/S0010218015003612>.
- [10] Løvås T, Mauss F, Hasse C, Peters N. Development of adaptive kinetics for application in combustion systems. *Proc Combust Inst* 2002;29(1):1403–10. [https://doi.org/10.1016/S1540-7489\(02\)80172-9](https://doi.org/10.1016/S1540-7489(02)80172-9). URL: <https://linkinghub.elsevier.com/retrieve/pii/S1540748902801729>.

- [11] Pepiot P, Automatic strategies to model transportation fuel surrogates, Ph.D. thesis; 2008.
- [12] Smith GP, Golden DM, Frenklach M, Moriarty NW, Eiteneer B, Goldenberg M, et al., GRI-Mech, <http://combustion.berkeley.edu/gri-mech/>.
- [13] Sung C, Law C, Chen J-Y. Augmented reduced mechanisms for NO emission in methane oxidation. *Combust Flame* 2001;125(1–2):906–19. [https://doi.org/10.1016/S0010-2180\(00\)00248-0](https://doi.org/10.1016/S0010-2180(00)00248-0). URL: <https://linkinghub.elsevier.com/retrieve/pii/S0010218000002480>.
- [14] Bahlouli K, Atikol U, Khoshbakhti Saray R, Mohammadi V. A reduced mechanism for predicting the ignition timing of a fuel blend of natural-gas and n-heptane in HCCI engine. *Energy Convers Manage* 2014;79:85–96. <https://doi.org/10.1016/j.enconman.2013.12.005>. URL: <https://linkinghub.elsevier.com/retrieve/pii/S0196890413007814>.
- [15] Gimeno-Escobedo E, Cubero A, Ochoa JS, Fueyo N. A reduced mechanism for the prediction of methane-hydrogen flames in cooktop burners. *Int J Hydrogen Energy* 2019;44(49):27123–40. <https://doi.org/10.1016/j.ijhydene.2019.08.165>. URL: <https://linkinghub.elsevier.com/retrieve/pii/S0360319919331830>.
- [16] Lu T, Law CK. A criterion based on computational singular perturbation for the identification of quasi steady state species: A reduced mechanism for methane oxidation with NO chemistry. *Combust Flame* 2008;154(4):761–74. <https://doi.org/10.1016/j.combustflame.2008.04.025>. URL: <https://linkinghub.elsevier.com/retrieve/pii/S0010218008002009>.
- [17] Jaravel T, Riber E, Cuenot B, Pepiot P. Prediction of flame structure and pollutant formation of Sandia flame D using Large Eddy Simulation with direct integration of chemical kinetics. *Combust Flame* 2018;188:180–98. <https://doi.org/10.1016/j.combustflame.2017.08.028>. URL: <https://linkinghub.elsevier.com/retrieve/pii/S0010218017303504>.
- [18] Chen J, Development of reduced mechanisms for numerical modelling of turbulent combustion, in: Workshop on Numerical Aspects of Reduction in Chemical Kinetics, CERMICS-ENPC Cite Descartes Champus sur Marne, France; 1997.
- [19] Humer S, Seiser R, Seshadri K. Experimental Investigation of Combustion of Jet Fuels and Surrogates in Nonpremixed Flows. *J Propul Power* 2011;27(4):847–55. <https://doi.org/10.2514/1.46916>. URL: <https://arc.aiaa.org/doi/10.2514/1.46916>.
- [20] Ranzi E, Frassoldati A, Stagni A, Pelucchi M, Cuoci A, Faravelli T. Reduced kinetic schemes of complex reaction systems: fossil and biomass-derived transportation fuels: reduced kinetic schemes of complex reaction systems. *Int J Chem Kinet* 2014;46(9):512–42. <https://doi.org/10.1002/kin.20867>.
- [21] <http://creckmodeling.chem.polimi.it/menu-kinetics/menu-kinetics-detailed-mechanisms>.
- [22] Zhu M. *Simulation aux grandes échelles du craquage thermique dans l'industrie pétrochimique*. These de doctorat de l'Université de Toulouse 2015:247.
- [23] Campet R, Simulation and optimization of steam-cracking processes, Ph.D. thesis; 2019.